iddrg

2015
Shanghai, China

Proceeding of the 34th International Deep Drawing Research Group

IDDRG 2015

May 31st – June 3rd ,2015

Shanghai , China

Edited by :

Shi-Hong Zhang

Ming Cheng

Juan Li

Yan Chen

Resolution requirements in time-dependent FLC testing

Roland Müller[a], Matthias Riemer[a], Patricia Weigel[a], Romy Petters[a], Peter Feldmann[b], Marko Schatz[b], Petra Aswendt[b]

[a]*Fraunhofer IWU Chemnitz*

[b]*ViALUX Messtechnik + Bildverarbeitung GmbH Chemnitz*

Corresponding author. Dr.-Ing.: Tel: +49 371 53971464; Fax: +49 371 539761464

E-mail addresses: roland.müller@iwu.fraunhofer.de

Abstract. For evaluation of the formability of sheet metal parts the forming limit diagram (FLD) is a valuable and generally used tool. The formability of the given sheet metal material in the FLD is represented by the forming limit curve (FLC). Typically FLCs are determined experimentally by standardized *Nakajima* tests using optical strain analysis systems. Other studies detected a huge influence of virtual facet size by stochastic patterns on the determined FLC values in time-dependent evaluation of FLC tests. In this paper the influence of the grid size of square line grids evaluated with the time-dependent method using the strain analysis system AutoGrid® is studied and compared with results from the evaluation of stochastic patterns with high local resolution using the ARAMIS system. The algorithm for time-dependent evaluation of the GDDRG Working Group has been applied for automatic detection of material failure and determination of FLC values. These studies are made for steel as well as aluminum sheet metal materials typically used for car body applications. Different methods and local grid resolutions were investigated for each material and compared with each other. Additionally a comparison between the time-dependent and the section based evaluation of the *Nakajima* FLC test is carried out. Furthermore all results are double-checked by visual operator´s control concerning the beginning of visible local necking. The experimental results show no significant difference between evaluation of 1 mm and 2 mm square line grids. Furthermore the FLC results evaluated with the AutoGrid® system (1.0 mm as well as 2.0 mm grid size) fit to the results rated by ARAMIS system using approximately 0.5 mm virtual grid size.

Keywords: deep drawing, FLC test, formability, strain measurement

Introduction

For the prediction of the feasibility for sheet metal parts, finite element method (FEM) is used. The precision of the simulation results strongly depends on the used material and process parameters [1]. The forming limit curve (FLC), where the onset of local instable necking is described as a function of major and minor strains, is commonly used as a failure criterion in FEM simulation as well as in evaluation of results of strain analysis in real forming processes. The Concept of forming limit curve was first developed by KEELER and GOODWIN [2,

3]. The FLC´s are usually obtained experimentally by Nakajima or Marciniak tests. The standardization for this testing method is given in ISO 12004 [4]. FLC testing results are influenced by the experimental setup, e.g. specimen geometry or lubrication and the evaluation method for detecting the onset of local necking [5, 6]. Actually, different methods are used for detecting the onset of local necking. In [7] the methods are distinguished in 0d-, 1d- and 2d-methods. The last state before crack is evaluated by the 0d-method and the achieved maximum principal strain is taken as the critical strain value. This approach is influenced by the user. The suggested method in ISO 12004 is the cross section method (1d-method). Therefore, in the last state before crack the strain distribution is evaluated along a cross section. An inverse parabola will be fitted in a defined fitting window to the measured strain distribution. The maximum of this parabola defines the major forming limit strain [4]. However, the accuracy of this method is controversial especially for high strength steel [8]. In this regard, the time dependent evaluation method (2d-method) is discussed in the German GDDRG FLC ISO 12004 working group.

The time dependent method is based on the analysis of the strain rate evolution in the region of necking. For the time dependent method a few approaches are in discussion [9]. The most important time dependent methods are the correlation coefficient method, the gliding correlation coefficient method, gliding difference of mean to median method and the linear best fit method [10]. In this investigation only the linear best fit method has been used for time dependent FLC test evaluation. This method is based on the analysis of the thinning rate as a function of time. The beginning of instable necking shows a strong raise of the thinning rate. In the stable stage and the instable stage two lines are fitted to the thinning rate curve. The crossing of the two lines is defined as the point of onset of instable local necking. For obtaining the critical major and minor strains the strain values are interpolated. [7] The linear best fit method is shown in Figure 1.

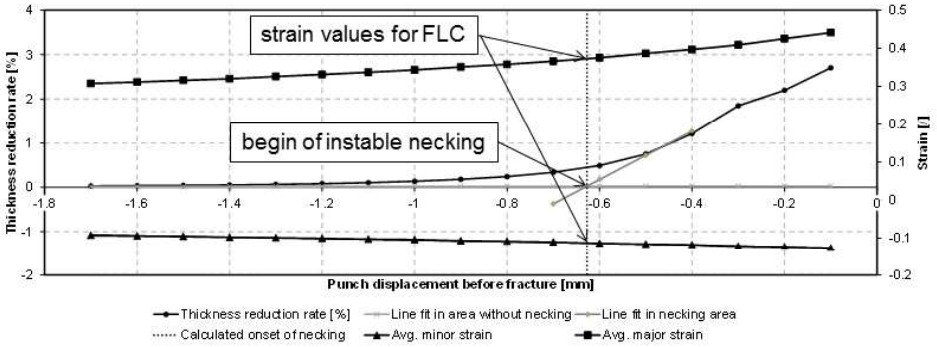

FIGURE 1. Linear best fit method

A study evaluated the influence of virtual grid size by stochastic patterns using the ARAMIS system on the determined FLC values in time dependent evaluation of FLC tests with the linear best fit method [11]. Therein the determined major strain values are significantly higher for a smaller virtual grid size [11].

In this paper the influence of the grid size of square line grids evaluated with the time dependent linear best fit method, is investigated and compared with stochastic pattern results with small virtual gird size. Furthermore the results being evaluated with the linear best fit method are compared to results evaluated with the cross section method. Additionally, all results are double-checked by visual operator´s control concerning the beginning of visible local necking.

Experimental Procedure

In the investigation two different materials were used. For the class of steels with high formability the steel grade DX54 and for the class of lightweight materials the aluminum alloy AA6014 was chosen. Both materials have a thickness of 1.0 mm. Table 1 shows the mechanical properties of the two materials.

TABLE 1. Tensile properties for the tested materials

Material	Yield Strength [MPa]	Ultimate Strength [MPa]	Ultimate Strain [%]
DX54	171	292	44,5
AA6014 T4	135	247	24,5

Note: All values are the mean of three repeats (sheet thickness 1 mm, 0° rolling direction).

The FLC tests were performed with an Erichsen sheet metal testing machine (145-60) and a tool for Nakajima testing according to DIN EN ISO 12004 [4]. The machine has a maximum drawing force of 600 kN and a maximum blank holder force of 250 kN. The tests were performed with 200 kN clamping force without the usage of a draw bead. A hemispherical punch with a diameter of 100 mm was used. Three different sample geometries were investigated to realize three different ratios of major and minor strains. Figure 2 shows a typical FLC and the three used sample geometries with different blank widths w_1=30 mm (A), w_2=90 mm (C) and w_3=200 mm (E). For each experimental setup three samples were tested. The tests were applied with a punch velocity of approximately 1 mm/s. The sample geometries were manufactured by using EDM (electrical discharge machining). For reduction of friction between the punch and the specimen a lubrication system according to [4] was used. The applied system is a layered stack of PTFE, drawing additive, soft PVC, Lanolin and PTFE.

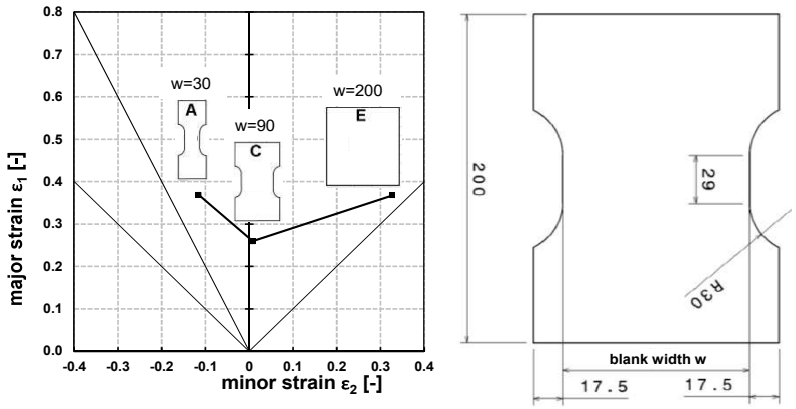

FIGURE 2. Schematic FLC with the three used sample geometries for Nakajima test (left) and a detailed drawing for the sample geometry (right)

For the strain measurement two different optical measuring systems were used. To evaluate the samples with square line grid pattern the AutoGrid® system (ViALUX) was used. This system is based on the automatic evaluation of grid patterns, which typically are electrochemically etched on the sample. To investigate the influence of the real grid size by time-dependent FLC determination, two square line grid patterns with a grid size of 1 mm and 2 mm were used (Fig 3). The forming process was recorded with a frequency of 10 Hz. In order to compare the test results carried out with the square line grid pattern, the same tests were performed with a stochastic pattern and a small virtual grid size setting with ARAMIS 12M (GOM) system (Fig. 3). Therefore the forming process was recorded with a frequency of

10 Hz too. For all measurements with the ARAMIS system the facet size was about 0.510 mm and the overlapping area was about 0.107 mm. All measurements were evaluated according to the linear best fit method. In the evaluation software for both measuring systems (AutoGrid® and ARAMIS) an implemented macro for the linear best fit method is available and was applied. The last 40 stages/picture sets before crack were used in both macros. For the evaluation with the cross section method also an implemented macro in AutoGrid® was used.

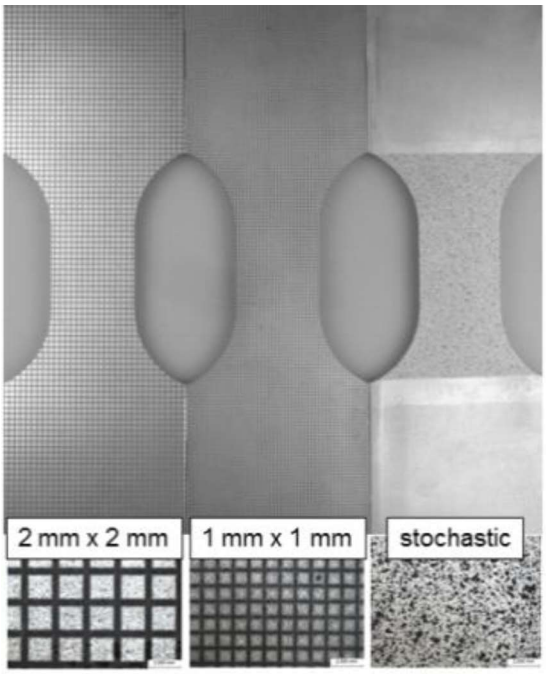

FIGURE 3. Sample geometries with w=30 mm and three different patterns for optical strain measurement

Results

In the Nakajima test all specimens were tested until fracture. For all specimens the fracture occurs in the apex of the dome as claimed in the DIN EN ISO 12004 (F).

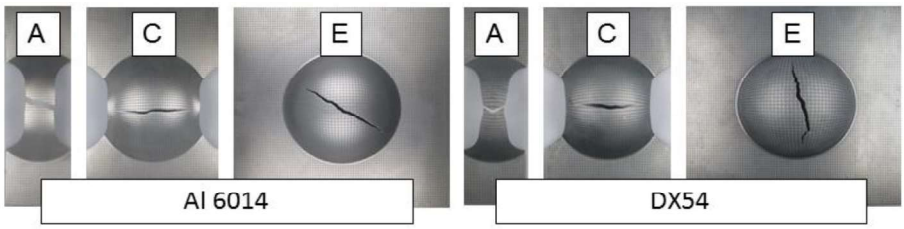

FIGURE 4. Fractures of the different sample geometries and materials

In Figure 5 the results for the material DX54 were depicted. For the three sample geometries evaluated with the line fit method critical strain values for 1 mm grid size were compared with critical strain values for 2 mm grid size. The results show no significant influence of the grid size to the critical major and minor strains for uniaxial tension, plain strain and biaxial tension for the material DX54. The average strain values for the three sample geometries were given in Table 2. In the column “range” the difference between the maximum and minimum value from the three samples is displayed. The range is also plotted in Figure 7. This value

quantifies the repeatability of the measurement and shows that there is no significant difference between the two investigated grid sizes. Furthermore, the difference between the average strain from the 1 mm and 2 mm grid was calculated. The analysis of the results has shown that this difference is in the same dimension as the value distribution at three samples from the same grid size. These differences mainly result from the variance of the material properties.

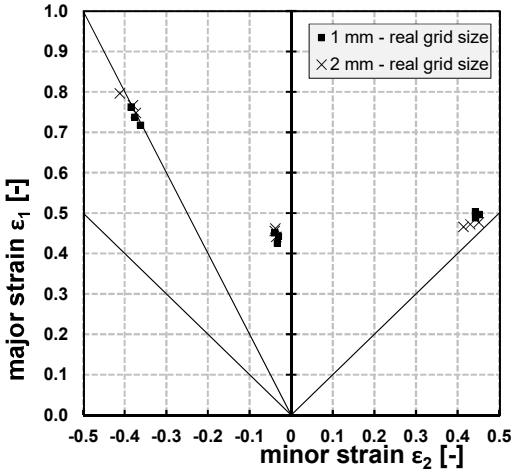

FIGURE 5. Major and minor strain values for the DX54 and two real grid sizesG

TALBE 2. Average strain values for the material DX54

specimen shape	grid size [mm]	average strain values*		range (ε_{imax} - ε_{imin})*	
		ε_1 [/]	ε_2 [/]	ε_1 [/]	ε_2 [/]
A	1	0.739	-0.385	0.045	0.022
A	2	0.748	-0.372	0.048	0.039
difference between the grid sizes		**0.009**	**0.013**	/	/
C	1	0.440	-0.034	0.025	0.009
C	2	0.453	-0.036	0.021	0.003
difference between the grid sizes		**0.013**	**0.002**	/	/
E	1	0.496	0.446	0.015	0.008
E	2	0.472	0.432	0.011	0.037
difference between the grid sizes		**0.021**	**0.014**	/	/

Note: All values marked with * are calculated of three repeats.

The results for the tested aluminum alloy AA6014 were shown in Figure 6. The comparison between the two grid sizes shows no significant difference between the evaluated values. The maximum difference of the major strain values between the two grid sizes occurs for the uniaxial tension with a value of 0.052.

The average strain values of three sample geometries obtained by Nakajima stretching are given in Table 3. The same parameters, which were presented for the material DX54 in Table 2, are shown in this table for the alloy AA6014. The range is nearly the same for both grid sizes. The difference between the average strain values were also calculated for the 1 mm and 2mm grid size. The analysis of the results has shown that this difference is in the same dimension as the value distribution at three samples from the same grid size. Table 2 and Table 3 show, that the differences of the average values of 1 and 2 mm grids are very small and there is no clear tendency: Sometimes average values of 1 mm grids are higher and sometimes those from 2 mm grids.

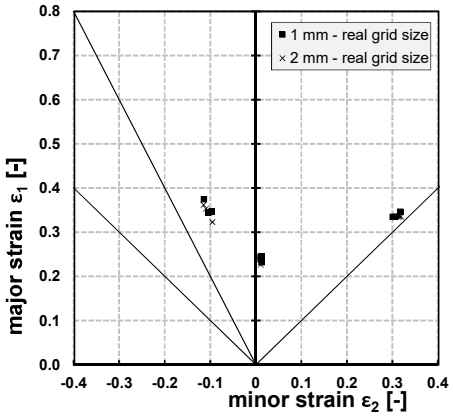

FIGRUE 6. Major and minor strain values for the AA6014 and two real grid sizes

TABLE 3. Average strain values for the material AA6014

specimen shape	grid size [mm]	average strain values*		range (ε_{imax} - ε_{imin})*	
		ε_1 [/]	ε_2 [/]	ε_1 [/]	ε_2 [/]
A	**1**	0.355	-0.105	0.045	0.023
A	**2**	0.346	-0.106	0.048	0.039
difference between the grid sizes		**0.009**	**0.001**	/	/
C	**1**	0.239	0.011	0.025	0.009
C	**2**	0.237	0.009	0.020	0.004
difference between the grid sizes		**0.002**	**0.002**	/	/
E	**1**	0.338	0.308	0.015	0.008
E	**2**	0.335	0.316	0.011	0.037
difference between the grid sizes		**0.003**	**0.008**	/	/

To compare the values from the samples with square grid pattern the same materials and specimen geometries were tested with a stochastic pattern and evaluated with ARAMIS system also with the linear best fit method. The average strain values from three samples are shown in Table 4. The range of the measured values lies in the same dimension compared to the square grid line pattern for the AA6014. However, the range calculated for the DX54 with stochastic pattern is approximately more than two times higher than the calculation for the AA6014 with stochastic pattern. This relation could not be seen at the square grid line samples. Moreover, the range of the strain values for the DX54 with stochastic pattern is higher than the range evaluated by the square line grid pattern. The big range by the DX54 with the stochastic pattern could occur caused by the high critical strains, which results in a failure of the stochastic pattern. For some specimens cracks in the marking color layers became visible.

TABLE 4. Average strain values for both materials evaluated with Aramis

specimen shape	*virtual grid size [mm]*	*average strain values**		*range (ε_{imax} - ε_{imin})**	
		ε_1	ε_2	ε_1	ε_2
A – DX54	0.5	0.833	-0.407	0.076	0.025
C – DX54	0.5	0.484	-0.045	0.053	0.008
E – DX54	0.5	0.478	0.394	0.036	0.07
A – AA6014	0.5	0.369	-0.116	0.024	0.01
C – AA6014	0.5	0.259	0.008	0.026	0.002
E – AA6014	0.5	0.368	0.331	0.005	0.019

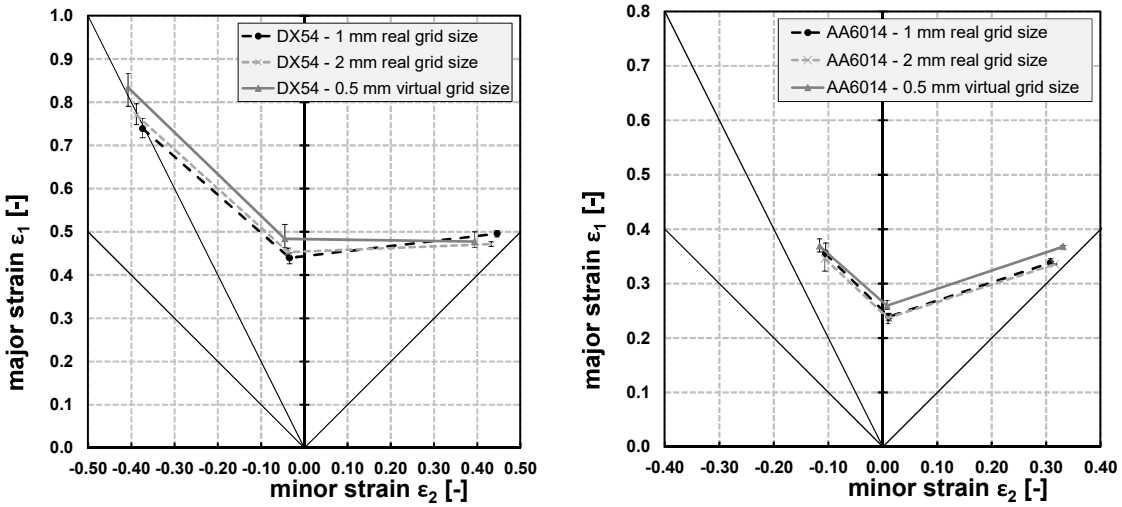

FIGURE 7. Comparison between the investigated grid sizes for DX54 (left) and AA6014 (right)

Figure 7 shows the FLC for the two materials and the three investigated grid sizes. The ranges of the mean values are also plotted in Figure 7. As explained above the curves for the different square grid sizes are in plausible agreement for both materials. The forming limit curve of the AA6014 with stochastic pattern has higher major strain values than the curves with the square line grid, but within the existing range of the results. As shown in Figure 7, the major strain values for the sample geometries A and C have a wide range, but the mean values are higher for the material DX54 using the stochastic pattern, but for shape E they are smaller than those from square line grids So there is no clear tendency, they are more or less the same.

For assessing the results of the linear best fit method a comparison with the cross section method were realized. Furthermore the results of the linear best fit method are double-checked by visual operator´s control concerning the beginning of visible local necking. This is exemplary shown for one specimen geometry (E) for the DX54 material with 2 mm real grid size. The 1 mm and 2 mm real grid size specimens for the two materials were evaluated with the cross section method. The results are shown in figure 8. As expected, the major strain values evaluated with the cross section method are below the strain values evaluated with the linear best fit method. It could be found no significant difference between the 1 mm and 2 mm real grid size for the cross section method by the AA6016 material.

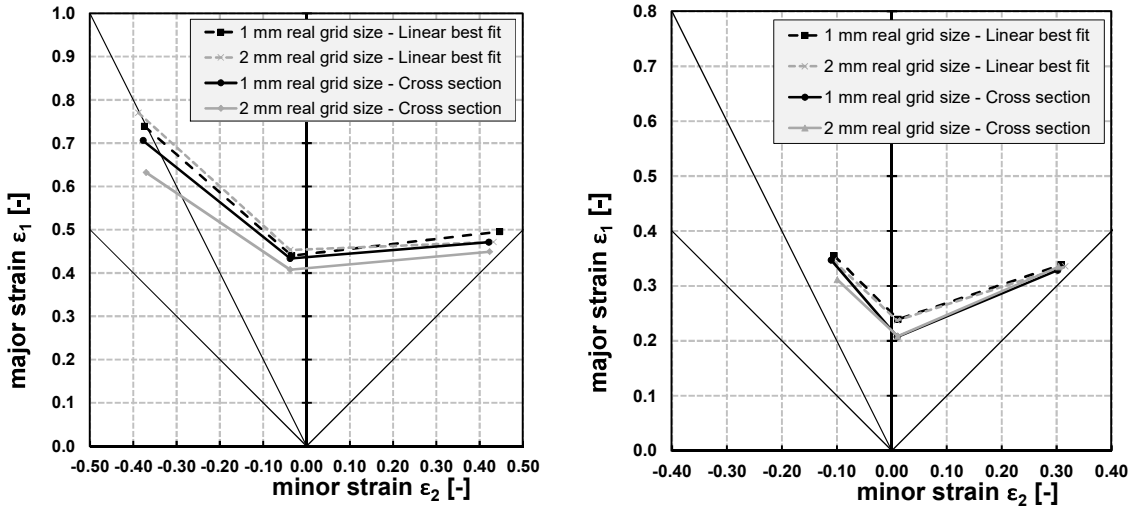

FIGURE 8. Comparison between the linear best fit method and the cross section method for DX54 (left) and AA6016 (right)

Following, the results of the double checking by visual operator's control for the specimen geometry E for DX54 material with 2 mm real grid size are given. The onset of local necking was calculated with the time dependent method to -0.64 mm punch displacement (Fig. 9). The pictures before (-0.7 mm punch displacement) and after (-0.6 mm punch displacement) the calculated point were visually checked by the operator for visible necking. On both pictures no necking could be found (Fig. 10). The first visible necking could be seen at -0.3 mm punch displacement (Fig. 10).

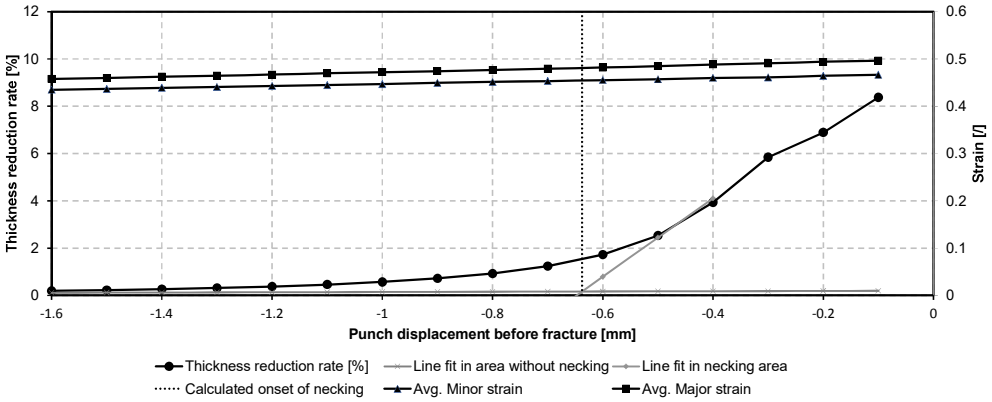

FIGURE 9. Result of the linear best fit method for the specimen geometry E for the DX54 material with 2 mm real grid size

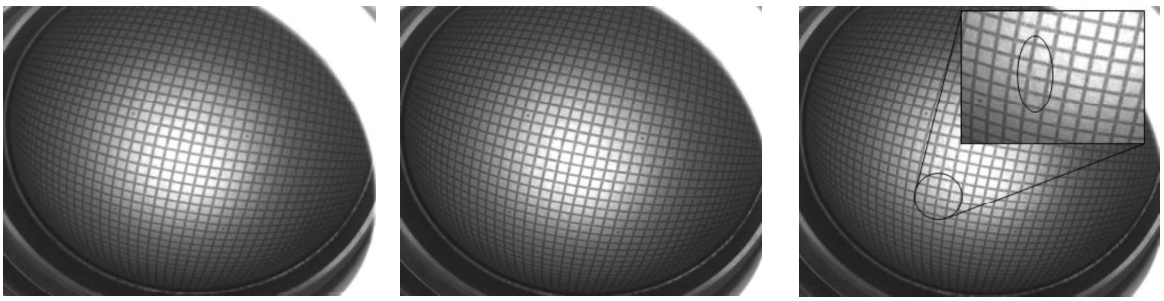

Punch displacement: -0.7 mm Punch displacement: -0.6 mm Punch displacement: -0.3 mm

FIGURE 10. Specimen E at different punch displacements

Conclusions

This presentation reports about investigation of the influence of grid size on the results of FLC determination with the time dependent linear best fit method. Additionally the results were compared with stochastic pattern using a virtual grid size of 0.5 mm evaluated in the same time dependent way. The difference between the FLCs performed with 1 mm and 2 mm grid size is not significant for the investigated materials. The comparison with the virtual grid size of 0.5 mm fit to the results evaluated with the square line grid patterns. The differences between the mean values evaluated with the different patterns for the DX54 as well as for AA6014 are in the variance of the tests. There is no clear differing tendency. All results are more or less in the same range.

As expected the major strain values evaluated with the cross section method systematically are a little bit lower than the values evaluated with the time dependent linear best fit method. The results from the linear best fit method are confirmed by visual operator´s control. No local necking is visible at the determined last image set before start of local necking determined by the linear fit method.

REFERENCES

1. Birkert, A.; Haage, S.; Straub, M.: Umformtechnische Herstellung komplexer Karosserieteile. Auslegung von Ziehanlagen. In: Umformtechnische Herstellung komplexer Karosserieteile (2013).
2. S. P. Keeler; W. A. Backofen: Plastic instability and fracture in sheets stretched over rigid punches. In: Trans. Am. Soc. Met. 56 (1963) 1, S. 25–48.
3. G. M. Goodwin: Application of strain analysis to sheet metal forming problems in the press shop. In: SAE Technical Paper 680093 (1968).
4. DIN Deutsches Institut für Normung e.V.: Metallische Werkstoffe - Bleche und Bänder - Teil 2Bestimmung der Grenzformänderungskurven im Labor 77.040.10 (2009) 12004-2. Berlin.
5. Dilmec, M.; Halkaci, H. S.; Ozturk, F.; Livatyali, H.; Yigit, O.: Effects of sheet thickness and anisotropy on forming limit curves of AA2024-T4. In: The International Journal of Advanced Manufacturing Technology 67 (2013) 9-12, S. 2689–700.
6. Hasek, V. V.: Untersuchungen und theoretische Beschreibungen wichtiger Einflussgrößen auf das Grenzformänderungsschaubild. In: Blech Rohre Profile 25 (1978) 5, S. 213–20.
7. Volk, W.; Hora, P.: New algorithm for a robust user-independent evaluation of beginning instability for the experimental FLC determination. In: International Journal of Material Forming 4 (2011) 3, S. 339–46.
8. Daamen, J.; Ingendahl, T.; Dahmen, K.; Meurer, M. (Hrsg.): Time dependent FLC determination of austenitic steels 2014.
9. Kuppert, A.; Merklein, M.; Friebe, H.; Möller, T.; Hotz, W.; Volk, W.: Einfluss der Auswertestrategie auf die Grenzformänderungskurve∗. In: Materials Testing 55 (2013) 9, S. 668–72.
10. Hotz, W.; Merklein, M.; Kuppert, A.; Friebe, H.; Klein, M.: Time Dependent FLC Determination Comparison of Different Algorithms to Detect the Onset of Unstable Necking before Fracture. In: Key Engineering Materials 549 (2013), S. 397–404.
11. Abspoel, M.: Influence of virtual grid size on FLC measurements with ARAMIS. Düsseldorf 2013.